



Published in final edited form as:

J Comp Neurol. 2018 August 01; 526(11): 1760–1776. doi:10.1002/cne.24445.

Architectonic characteristics of the visual thalamus and superior colliculus in titi monkeys

Mary KL Baldwin and Leah Krubitzer

Center for Neuroscience, University of California, 1544 Newton Court, Davis, CA 95618

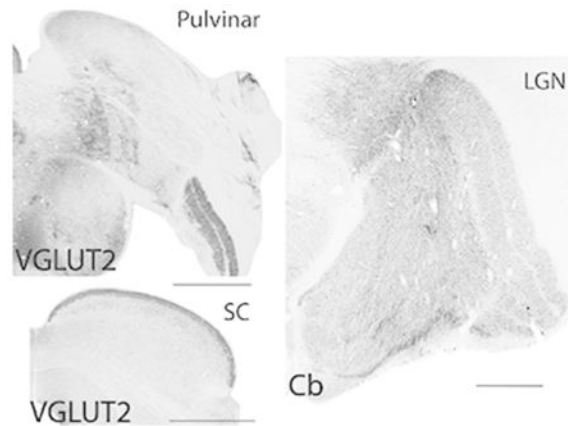
Abstract

Titi monkeys are arboreal, diurnal New World monkeys whose ancestors were the first surviving branch of the New World radiation. In the current study, we use cytoarchitectonic and immunohistochemical characteristics to compare subcortical structures associated with visual processing with those of other well-studied primates. Our goal was to appreciate features that are similar across all New World monkeys, and primates in general, versus those features that are unique to titi monkeys and other primate taxa. We examined tissue stained for Nissl substance, cytochrome oxidase (CO), acetylcholinesterase (AChE), calbindin (Cb), parvalbumin (Pv), and vesicular glutamate transporter 2 (VGLUT2) to characterize the superior colliculus, lateral geniculate nucleus, and visual pulvinar. This is the first study to characterize VGLUT2 in multiple subcortical structures of any New World monkey. Our results from tissue processed for VGLUT2, in combination with other histological stains, revealed distinct features of subcortical structures that are similar to other primates, but also some features that are slightly modified compared to other New World monkeys and other primates. These included subdivisions of the inferior pulvinar, sublamina within the stratum griseum superficial (SGS) of the superior colliculus, and specific koniocellular layers within the lateral geniculate nucleus. Compared to other New World primates, many features of the subcortical structures that we examined in titi monkeys were most similar to those in owl monkeys and marmosets, with the lateral geniculate nucleus consisting of two main parvocellular layers and two magnocellular layers separated by interlamainar zones or koniocellular layers.

Graphical abstract

Architectonic analysis of subcortical visual structures of the titi monkey provide insights into the evolution of the organization and functional characteristics of different visual streams in primates. Coronal titi monkey tissue sections of the pulvinar (top left), superior colliculus (bottom left), and lateral geniculate nucleus (right) stained for vesicular glutamate transporter 2 (VGLUT2) or calbindin (Cb). Lateral is the right, dorsal is up, scale bar is 1 mm.

*Correspondence to: Mary K L Baldwin, University of California, Davis, Center for Neuroscience, 1544 Newton Court, Davis, CA 95618, Phone: 530 757 8560, Fax: 530 757 8827, mkbaldwin@ucdavis.edu.



Keywords

evolution; primate; New World monkey; visual pathways; RRID AB_287552; RRID 2313581; RRID AB_10000347; RRID AB_477329

Introduction

A majority of knowledge of the visual system in New World monkeys comes from four species: owl monkeys, capuchin monkeys, squirrel monkeys, and marmosets. Each of these species has a unique lifestyle, eye morphology, and visually mediated behavior that would make some aspects of their visual system unique from other primates, including humans. For instance, owl monkeys are nocturnal (Fleagle, 2012), and therefore have secondarily acquired retinal specializations associated with nocturnal vision (Koga et al., 2017). These include an increase in eye size, changes in the cellular composition of the retina (Dyer et al., 2009), and the loss of S cones necessary for color vision (Jacobs et al., 1996). Ultimately, these alterations, along with their nocturnal lifestyle, could impact the organization of subcortical structures of the visual system that are specialized for color vision. The capuchin monkey has a pseudo-thumb (Almécija and Sherwood, 2017), allowing it to use tools and adjust reaching and grabbing behaviors in unique ways compared to other New World monkeys (Visbalerghe et al., 2015; Managalam and Frigaszy, 2015). This ability has resulted in changes to parts of the brain devoted to hand use and visual-manual behaviors (Padberg et al., 2007). Marmosets have multiple adaptations, including a decreased body size, the reintroduction of claws vs. nails on the digits for vertical climbing, and reduced eye movement capabilities with accompanied head cocking (Kaplan and Rogers, 2006; Jackson, 2011). Squirrel monkeys also engage in head cocking (Rumbaugh, 1968), and have a small ocular motor range and interocular distance which affect head movements during visual search (McCrea and Gdowski, 2003). These morphological and behavioral changes associated with diverse lifestyles in different New World monkeys have likely had an effect on the visual system, including visual perception, hand-eye coordination, and visually guided reaching and grasping. Despite these differences, comparative studies indicate many similarities between the features of their visual systems due to retention from a common ancestor.

The comparative method, using cladistics as a guide, can be an exceptionally powerful tool for providing an understanding of which features of the brain are likely homologous versus those that are unique to a given species (derived). However, in best practice, this technique relies on a broad survey of the features in question of both closely related species, as well as more distant relatives. When a similar feature of brain organization is present in a large group of related animals, principles of parsimony indicate that it was present in their common ancestor and is therefore homologous. However, in order to make accurate inferences about homologous versus derived features, it is necessary to examine multiple species. The more species examined the more accurate the inference, not only about the ancestral form, but about extant species that cannot be studied with invasive techniques, such as humans.

The current study examines the histological characteristics of subcortical visual structures in New World titi monkeys (*Callicebus moloch*). Titi monkeys are diurnal arboreal primates dispersed throughout much of South America, with *Callicebus moloch* located in northern Brazil (Hershcovitz, 1988). Titi monkeys are one of a small percentage of mammals, and the best available primate model, that are socially monogamous and engage in pair bonds that last a lifetime (Bales et al., 2017 for review). Current evidence suggests that they shared a common ancestor with other New World monkeys about 25 million years ago (Perelman et al., 2011; Springer et al., 2012), but their lineage was the first to diverge from the New World line (Fig. 1). Because of their phylogenetic status, it is possible that many of the brain features present in titi monkeys reflect those that have been retained from the common ancestor of New and Old World monkeys. Therefore, data obtained from titi monkeys may allow for more robust comparisons and more accurate inferences about the evolution of the visual system in primates.

We chose specific histological stains to study subcortical visual structures including the superior colliculus, lateral geniculate nucleus, and pulvinar nucleus. Combined, these subcortical structures comprise multiple functionally distinct visual pathways in which information from the retina reaches visual cortex (see Baldwin and Bourne, 2017; Casagrande and Khaytin 2009; Kaas and Huerta, 1988 for reviews). In studies of New World monkeys and other primates, some immunohistological preparations have been found to reveal specific pathways, or parts of pathways, within the visual system. For instance, the calcium binding proteins parvalbumin and calbindin have often been associated with different functional streams within the visual system, especially with respect to those traversing the lateral geniculate nucleus (Casagrande 1994; Goodchild and Martin, 1998; Jones, 2007; Casagrande and Khaytin 2009). These proteins have also been useful in identifying subdivisions of the pulvinar in some primates (i.e. Cusick et al., 1993; Stepniewska and Kaas, 1997; Gutierrez et al., 1995; Warner et al., 2010). Vesicular glutamate transporter 2 (VGLUT2) is responsible for transferring glutamate into presynaptic vesicles of glutamatergic neurons across the central nervous system and has been associated with excitatory inputs from subcortical structures (i.e. Balaram et al., 2011; 2013; Rovo et al., 2012). Importantly, tissue processed for VGLUT2 protein expression reveals specific subdivisions of the pulvinar that are not always apparent in other histological stains, such as calbindin (Baldwin et al., 2013; Baldwin et al., 2017). The subcortical visual structures have not been studied using VGLUT2 immunohistological preparations in New World monkeys

(except for the pulvinar in squirrel monkeys, Baldwin et al., 2017), but have been used to study the superior colliculus, lateral geniculate nucleus, and pulvinar complex of galagos (Balaram et al., 2011), macaques (Balaram et al., 2013), as well as tree shrews and squirrels (Baldwin et al., 2011; Balaram et al., 2015). These immunohistological stains were used in conjunction with more classical architectonic staining procedures such as cytochrome oxidase (CO), Nissl, and acetylcholinesterase (AChE), to reveal thalamic borders, the laminar organization of the superior colliculus and the lateral geniculate nucleus, as well as subdivisions of the pulvinar. Thus, our intention was to use a variety of histological markers to make comprehensive comparisons of the architectonic features of the superior colliculus, lateral geniculate nucleus, and pulvinar across New World monkeys and other primate lines.

Materials and Methods

The brains of three titi monkeys (*Callicebus moloch*) were used in the current study (see Table 1 for details). All procedures were carried out in accordance to the NIH *Guide for the Care and Use of Laboratory Animals*, and were reviewed and approved by the University of California, Davis Institutional Animal Care and Use Committee.

Tissue acquisition

Animals were given a lethal dose of sodium pentobarbital and were perfused transcardially with 0.1 M phosphate buffered saline (PBS) followed by 2% paraformaldehyde (2% PFA), and then 2% PFA with 10% sucrose added. The brainstem and thalamus were then separated from overlying brain structures (Fig. 2b and c). All tissue was post fixed in 4% PFA for 1–24 hours and then placed in a 30% sucrose solution for 24–48 hours. The thalamus and brainstem were cut coronally at 50 μm on a freezing microtome.

Histological processing

Tissue sections were saved in series of 5 (see Table 1 for specific details). Series processed for Nissl (Crystal violet), cytochrome oxidase (CO: Wong-Riley, 1979), or acetylcholinesterase (AChE: Geneser-Jensen and Blackstand, 1971) staining were used as references for architectonic boundaries of visual structures. Other series were sent through immunohistochemical processing for calbindin (Cb), vesicular glutamate transporter 2 (VGLUT2), or parvalbumin (Pv) to define distinctions within the layers of the superior colliculus and lateral geniculate nucleus, and subdivisions of the pulvinar.

Immunohistology for VGLUT2, Cb, and Pv used commercial antibodies against each protein (see Table 2 for details). Sections were post-fixed for one hour in 4% PFA and rinsed in 0.01 M PBS. Endogenous peroxide activity was quenched with 0.01% hydrogen peroxide in 0.01 M PBS for 10 minutes. Sections were then rinsed in PBS, incubated in blocking solution (5% normal horse serum and 0.05% triton in 0.01 M PBS) for two hours. After this time, sections were transferred into the desired concentration of primary antibody (Table 2) in blocking solution and placed on a rocker at 4 °C for 48 hours or at room temperature for 24 hours. Sections were then rinsed three times in 0.01 M PBS, then transferred into a blocking solution with the secondary antibody (see Table 2) for 1.5–2 hours at room temperature. Sections were rinsed three times and then incubated overnight at 4 °C in avidin/

biotin-peroxidase complex solution (ABC kit, Vector Labs). Sections were rinsed three times in PBS and then reacted in a 0.1% 3'3' diaminobenzidine, 0.001% hydrogen peroxide, and 0.02% nickel ammonium sulfate solution in 0.1 M PB to visualize the stain.

Antibody Characterization

Table 2 outlines the antibodies used in the current study. Control tissue sections were processed using the procedures outlined above with primary antibodies omitted. No labeling for VGLUT2, Cb, or Pv was observed in control sections.

Imaging and analysis

Digital photographs of the uncut titi monkey brain were captured with a Nikon (DSLR 5200) digital camera. Photomicrographs of tissue sections were captured using a Microfire camera (Optronics, Goleta, CA) mounted to a Nikon E400 microscope or an Aperio ScanScope. Images were cropped and adjusted for brightness and contrast with Adobe Photoshop, but were otherwise unaltered.

Terminology

Diverse terminology has been used to denote the different layers of the lateral geniculate nucleus in different laboratories and different species. Here we adopt the convention first introduced by Kaas et al., 1978 for defining the magnocellular and parvocellular layers for internal (MI or PI) and external lamina (ME or PE), while using the numbering system within the K layers introduced by Casagrande (see Casagrande et al., 2007 for review).

Results

The superior colliculus

The superior colliculus (SC) is a midbrain structure located caudal to the thalamus (Fig. 2b and c). Similar to other primates, the superior colliculus of titi monkey is well-laminated and composed of seven main layers. These layers include the stratum zonale (SZ), stratum griseum superficiale (SGS), stratum opticum (SO), stratum griseum intermedium (SGI), stratum album intermedium (SAI), stratum griseum profundum (SGP), and stratum album profundum (SAP). We focus mainly on the superficial layers of the superior colliculus, as these layers are involved in visual processing, while deeper layers are involved in multisensory integration and motor functions (May, 2006).

The stratum zonale, SZ, is often divided into two layers in other primates (Balaram et al., 2013), with the most superficial layer containing mostly astrocytes and the lower layer containing mostly fibers (Lund, 1972). The most dorsal layer stains weakly for CO, Cb neuropil, and VGLUT2, while the other layer stains darkly for CO, Cb neuropil, and VGLUT2, often appearing as a dark band just above the SGS (Fig. 3).

The SGS is a cell dense layer that stains darkly for CO, with the upper SGS staining homogeneously dark, while the lower SGS stains slightly lighter (Fig. 3b). The pattern of VGLUT2 staining was not consistent within the upper SGS throughout the full extent of the superior colliculus (Fig. 4). In more caudal locations, large, darkly staining terminals give

the upper SGS a uniformly dark appearance throughout the medial to lateral extent of the superior colliculus. On the other hand, in more rostral and medial locations the pattern of dark VGLUT2 staining within the upper SGS becomes patchy, and in some instances, two bands of darkly staining neuropil are visible (Fig. 4c). In the lower SGS the staining pattern is much lighter and VGLUT2 positive cells are present.

The density of cell bodies within the SO is slightly less than that in the SGS. The SO is only slightly lighter in CO, VGLUT2, and AChE preparations than the lower SGS mainly due to fibers of passage coursing through this layer. Distinguishing the SO from the SGI is somewhat difficult based on CO or VGLUT2 staining characteristics. The SGI has fewer large fiber tracks running through it, giving the SGI a somewhat more darkly staining and homogeneous appearance (Fig. 3). The difficulty in distinguishing the SO/SGI border is especially apparent within the medial vs. the lateral aspect of the SC (i.e. Fig. 3). However, the SGI does stain slightly more darkly for AChE (Fig. 3d), VGLUT2 (Fig. 3f), and CO (Fig. 3b) and contains slightly larger cell bodies than those found within the SO and more superficial layers (Fig. 3a). Cb preparations show little to no protein expression within neuropil, but a few small Cb positive (+) cells were scattered within the SGI (Fig. 3e). Pv + neuropil staining within the SGI progressively diminishes through the dorsal to ventral extent and large Pv + cells are scattered throughout the full depth of the SGI (Fig. 3c). The border between the SGI and SAI is distinct as the SAI stains weakly for CO, AChE, Pv, and VGLUT2.

The lateral geniculate nucleus

The layers of the lateral geniculate nucleus are traditionally defined based on their relative location and cell type. In titi monkeys, the lateral geniculate nucleus contains two magnocellular layers with the external magnocellular layer (ME) located ventrally. Dorsal to ME is the internal magnocellular layer (MI). At least two parvocellular layers (the internal (PI) and the external (PE) parvocellular layers) are located dorsal to MI (Fig. 5). In the present study, we refer to both the interlaminar layers and the small cell S laminae as koniocellular layers. At least four koniocellular (K) layers are also observed in titi monkeys. K1 is located along the most ventral aspect of the lateral geniculate nucleus between the optic tract and the external magnocellular (ME) layer. K2 lies between the two magnocellular layers, K3 is located at the border between the magnocellular and parvocellular layers, and K4 is often visible between the two parvocellular layers (Fig. 5).

In the Nissl stained sections, the magnocellular layers are marked by their large darkly staining cell bodies (Fig. 5c). These layers also stain more darkly for Pv (Fig. 5g). Cytochrome oxidase and AChE stained sections reveal the presence of fiber tracts coursing vertically through the magnocellular layers (Fig. 5e and h) giving them a somewhat striated appearance, especially within the medial aspect of the lateral geniculate nucleus. The parvocellular layers contain dense cell bodies that are smaller than those found in the magnocellular layers, but are larger than those observed in the koniocellular layers. The parvocellular layers are more homogeneous in their staining characteristics as they lack the fibers running through them that the magnocellular layers exhibit (Fig. 5g). Despite differences in the sizes of the cells that compose the magnocellular and parvocellular layers,

few differences were observed in other histological preparations with only CO and Pv showing slightly darker staining patterns within the parvocellular vs magnocellular layers (Fig. 5e and g).

The koniocellular (K), or interlaminar, layers were distinguished by small cell bodies in Nissl preparations, but were not particularly distinct in CO, Pv and AChE preparations (Fig 5e, g, and h). These layers were most obvious in VGLUT2 and Cb stained tissue sections. K1 is especially prominent in VGLUT2 and Cb stained sections as this layer stains much darker compared to other layers. Both the dark Cb+ neuropil and VGLUT2 portions of K1 seem to overlap with one another in position (Fig. 6). Both Cb+ neuropil and cell bodies were present in K1, K2 and K3 though the distribution of Cb+ neuropil was not consistent throughout K3. Some regions of the lateral geniculate nucleus had very little Cb+ neuropil (Fig. 6), while other sections had dense Cb+ neuropil. K3 also had VGLUT2 stained terminals, but they were less dense and more widely distributed compared to K1 and K2 (Fig. 6). The interlaminar zone between PI and PE (K4) stained weakly for both VGLUT2 and Cb. In AChE, Pv, and CO preparations, the interlaminar zone between PI and PE could not be identified (Fig. 5). Pv positive neuropil were present in P, M, and K layers, making distinctions of different layers based on this stain alone difficult (Fig. 5g).

The pulvinar

The pulvinar complex in titi monkeys is located along the most dorsocaudal aspect of the thalamus, lateral and rostral to the superior colliculus, and dorsal to the dorsal lateral geniculate nucleus (Fig. 2b and c). The pulvinar is composed of multiple divisions, including the inferior (PI), lateral (PL), medial (PM), and anterior (PA) pulvinar. In the present study, we focus primarily on the inferior and lateral pulvinar divisions. The inferior and lateral divisions share strong connections with cortical visual structures, receive input from the superficial layers of the superior colliculus (PIp and PIcm), and also receive direct projections from the retina (PIm) (See Baldwin et al., 2017; Baldwin and Bourne 2017; Bridge et al., 2016 for reviews).

Inferior pulvinar—The inferior pulvinar lies along the most caudal and medioventral aspect of the pulvinar complex. There are multiple subdivisions of the inferior pulvinar including the posterior (PIp), medial (PIm), central medial (PIcm), and central lateral (PIcl) divisions.

Architectonically, PIp and PIcm are very similar to one another in staining properties, with both nuclei staining darkly for Cb and VGLUT2; indeed, it appears that these two nuclei fuse together either at their dorsal or ventral aspects (see Figs. 7b, c, and 8). However, there are slight differences in their architectonic staining patterns. For instance, PIcm stains much more darkly for AChE (Fig. 7e) than PIp; however, PIp stains more darkly for CO than PIcm (Fig. 7d). PIp also contains larger cell bodies that are more spatially distributed than PIcm (not shown). Further, PIp stains more darkly and homogeneously for VGLUT2 than PIcm. Instead, PIcm appears to have a heterogeneous VGLUT2 staining pattern with the medial aspect of PIcm having dense clusters of VGLUT2 protein expression, while the more lateral aspect stains less densely. A region of weak VGLUT2 staining separates the medial from the

lateral PIcm in caudal sections, making it appear as if there are two VGLUT2 bands within this division (Figs 7c and 8c).

PIIm lies between PIp and PIcm. This nucleus is often characterized by a lack of Cb staining (Fig. 7b) and is thus often referred to as the “calbindin hole.” Though a few Cb+ cells are present within PIIm of titi monkeys (Fig 7b), Cb+ neuropil is lacking. VGLUT2 immunohistological staining also shows little to no VGLUT2 protein in this subdivision, except in locations where there appears to be interleaving connections between PIp and PIcm (Fig. 8b, and c). In AChE preparations (Fig. 7e), PIIm stains moderately, similar to PIp. PIIm and PIp are indistinguishable in CO preparations (Fig. 7d).

PIcl is often considered to be functionally associated with the lateral pulvinar, PL (Kaas and Lyon, 2007; Baldwin et al., 2017), but for historical consistency, PIcl is still considered to be within the inferior pulvinar. This subdivision is more clearly differentiated from PIcm by its relatively lighter VGLUT2 staining characteristics. There are subtle differences in AChE staining, with PIcl staining slightly darker for AChE than PIcm. Determining a border between PIcl and PIcm using Cb is difficult in titi monkeys.

The shell—An additional architectonic division, which we refer to as the shell (s), was apparent along the most lateral aspect of pulvinar of titi monkeys (Figs. 7 and 9). This division is present along the inferior half of the pulvinar along most of the caudal to rostral extent and shares borders with PIcl and PL (Figs. 7 and 9). At caudal locations, this division is narrow (Fig. 7), but it expands in width at more rostral locations, then recedes into the border with the lateral geniculate nucleus at its most rostral extent (not shown). The architectonic features of this division are reminiscent of the inferior lateral shell described in squirrel monkeys (Cusick et al., 1993; Gutierrez et al., 1995) with moderate AChE and dark Cb staining (Figs. 7 and 9). This division is distinct from PIcl by the visible vertical fiber tracts that course through it, which are revealed best in AChE preparations (not shown). A slight increase in VGLUT2 terminal label also helps differentiate this division from both PIcl and PL (Fig. 9c). We do not assign this division of the pulvinar to either the inferior or lateral pulvinar, but instead wish to keep open the possibility that this division of the pulvinar could belong to either, depending on its possible homologue in other primates and their close relatives.

Lateral pulvinar—The lateral pulvinar (PL) runs along the most lateral aspect of the pulvinar complex and is bordered dorsomedially by the medial pulvinar and ventromedially by the inferior pulvinar (Fig. 7). The lateral pulvinar of titi monkeys can be easily distinguished from the medial pulvinar (PM) in CO and AChE preparations as the medial pulvinar stains relatively weakly compared to the lateral pulvinar in these preparations (Figs. 7d, e and 9d, e). The medial pulvinar also stains slightly darker for VGLUT2 (Figs. 7 and 9). In sections processed for Nissl, the medial pulvinar is distinguished by densely packed and evenly distributed cells, while cells in PL are irregularly distributed between fiber tracks coursing horizontally through this division (not shown). Further, there is a population of large Cb+ cells that borders PL and PM, with cells dispersed between both divisions (Fig. 9b). The border between the lateral pulvinar and the inferior pulvinar is less apparent in rostral sections, but is most easily identified in AChE preparations, where the darkly staining

PIcm and PIcl contrast with the moderately staining PL (Fig. 9e). PL is not homogeneous in its histological staining properties. For instance, the dorsomedial aspect of PL has a much higher concentration of Cb+ neuropil and cells than the lateroventral aspect of PL (Fig. 9b). A distinction between these two regions is not apparent in other stains.

Discussion

In the present report, we describe the architectonic characteristics of the subcortical visual structures in New World titi monkeys including the superior colliculus, lateral geniculate nucleus, and visual pulvinar. We first discuss how the organization and staining properties of the superior colliculus, lateral geniculate nucleus, and pulvinar compare with those described in other New World monkeys, focusing on common features as well as those that appear to be unique to titi monkeys. Our objective is to make accurate inferences about the organization of the visual system of the common ancestor of all New World monkeys. In the second portion of this discussion we compare the organization of subcortical structures in New World monkeys with those in prosimians and the commonly used macaque monkey, with the overall goal of understanding how the visual system evolved and specialized in primates. Our comparative analysis of primates reveals that despite some differences in visual behaviors (nocturnal, diurnal, or crepuscular), eye size, retinal composition, and the use of the visual system to navigate and interact with the environment, there is remarkable conservation of the organization of visual thalamic nuclei and especially the superior colliculus. Probably the most noted derivation is related to the amount of the lateral geniculate nucleus devoted to processing parvocellular inputs in anthropoid primates, and the differences in the architectonic characteristics of the K layers. The second notable alteration to the thalamus is the extraordinary expansion of the pulvinar complex, which correlates well with the expansion of extrastriate cortex in primates, particularly in anthropoid monkeys.

Comparison to New World Monkeys

Superior colliculus—Surprisingly, the cytoarchitecture of the superior colliculus beyond that of Nissl or CO stains has not been well studied in New World monkeys, with the most comprehensive studies conducted in cebus monkeys using various calcium binding proteins (Soares et al., 2001a; 2003).

Generally, the superior colliculus in New World monkeys has seven layers which have a similar laminar pattern in Nissl and CO preparations. The SGS contains a dense cluster of cells that stain more intensely for CO relative to the SO. The SGI is distinguishable from the SO by having larger cells and more dense CO staining (Bourne and Rosa, 2003; Collins et al., 2005b). The contrast in both the density of cells and the intensity of CO staining does not seem as robust between the superficial layers and the SGI in titi monkeys relative to other New world monkeys, but quantification of cell number and staining density is required.

Calbindin staining in the superior colliculus of cebus monkeys reveals a dense layer of neuropil within the superficial portion of the SGS similar to titi monkeys. However, unlike titi monkeys, cebus monkeys have Cb+ cells within the SGS and SO (Soares et al., 2001a;

2003). Tissue processed for Pv antibodies in cebus monkeys reveals Pv+ cells distributed throughout the SGS, SO and SGI. In the SGS and SO, Pv+ cells were small to medium sized stellate neurons, while in the SGI they were large multipolar cells (Soares et al., 2001a; 2003). Though the pattern of retinal terminals has not been reported in titi monkeys, VGLUT2 staining within the superior colliculus (Figs. 3 and 4) has a similar pattern to that of the retinal termination patterns observed in the closely related squirrel monkey (Tigges and O'Steen, 1974; Tigges and Tigges, 1981).

Lateral geniculate nucleus—The architectonic organization of the lateral geniculate nucleus has been described in owl monkeys, cebus monkeys, squirrel monkeys, and marmosets (Kaas et al., 1978; Xu et al., 2001; Casagrande et al., 2007; Soares et al., 2008; Bourne and Rosa, 2003; Goodchild and Martin, 1998). In all of these species, magnocellular (M), parvocellular (P), and koniocellular (K) layers can be distinguished. Generally, the standard laminar pattern in New World monkeys (and primates in general) consists of two magnocellular layers and two parvocellular layers (Fig. 10). These two sets of magnocellular and parvocellular layers are further differentiated from one another based on their position. The external M layer (ME) lies next to the optic tract, while the layer just dorsal to this is the internal M layer (MI). Running along the dorsal border of the lateral geniculate nucleus is the external P layer (PE), while the internal layer (PI) is the layer adjacent to MI (Fig. 10). In some primates, the P layers split into interweaving leaflets. Thus, in some New World monkeys such as cebus (Soares et al., 2008) and squirrel monkeys (Kaas et al., 1978) it appears as if there are four P layers in some portions of the lateral geniculate nucleus. However, distinctions between P layers in squirrel monkeys, are not always easily observed unless retinal projections are revealed (Tigges and O'Steen, 1974; Kaas et al., 1978; Fitzpatrick et al., 1983).

An additional set of layers, the koniocellular (K) layers, are also found throughout all studied New World monkeys and all primates (see Kaas et al., 1978; Casagrande, 1994; Hendry and Reid, 2000; Casagrande and Xu, 2004, and Casagrande and Khaytin, 2007; Goodchild and Martin, 1998). However, the anatomical organization of these layers across primates, and even within New World monkeys, is varied (see Casagrande and Khaytin, 2007 for review). For instance, the existence of interlaminar layers between P layers in squirrel monkeys are often not reported (i.e. Kaas et al., 1978; Fitzpatrick et al., 1983; Tigges and O'Steen, 1974; Harting et al., 1991; Usrey and Reid, 2000).

There is some evidence that the different K layers within a given primate species have functionally distinct characteristics (White et al., 2001; Solomon et al., 2002; Xu et al., 2001) and connection patterns with cortical and subcortical visual structures (Casagrande and Xu, 2004; Stepniewska et al., 1999; 2000), including different inputs from the retina (Percival et al., 2014). Further evidence for functional differences comes from the variation of histological staining characteristics across the layers. For example, in owl monkeys, K1, K2, and K3 appear to contain the greatest number of cells labeled with calbindin, and the layer with the densest Cb+ neuropil is K1 (Xu et al., 2001), while there are almost no Cb+ cells in K4. In marmosets, calbindin reveals K1 and K3 layers within the lateral geniculate nucleus, while K2 has only a few to no Cb+ cells or neuropil (Goodchild and Martin, 1998; White et al., 2001; Warner et al., 2010).

The lateral geniculate nucleus of titi monkeys is similar to owl monkeys and marmosets, with two parvocellular and two magnocellular layers. Also, like the owl monkey, K1, K2, and K3 of titi monkeys all contain Cb+ cells, while K4, which lies between the P layers, does not. Furthermore, only K1 and K2 have dense Cb+ neuropil. VGLUT2 labeling in other New World monkeys has not been reported for the lateral geniculate nucleus. However, K1–K4 all have VGLUT2 terminal label, albeit in a progressively weaker pattern, with K1 having the densest terminal label, while K4 has the least dense VGLUT2 terminal label.

These differences in architectonic staining patterns suggest that each K layer might be functionally different, with some layers being more different than others. For instance, K1 and K2 are the most similar based on Cb and VGLUT2 staining patterns (Cb+ cells and neuropil and dense VGLUT2 staining), while K3 is less similar (Cb+ cells and moderate VGLUT2 staining) and K4 (only weak VGLUT2 staining) is the most dissimilar.

Visual pulvinar—The visual pulvinar includes the inferior and lateral divisions and has been described in owl monkeys, squirrel monkeys, cebus monkeys, and marmosets (see Baldwin and Bourne, 2017; Baldwin et al., 2017 for reviews and Soares et al., 2001). Our current understanding of the divisions of the inferior pulvinar of New World monkeys is derived from the seminal work of Lin and Kaas (1979; 1980) in owl monkeys. In their original study, PIcm and PIcl were given the name PIc. It was not until 1997 that AChE staining patterns in squirrel monkeys revealed that PIcm and PIcl were separate divisions of the inferior pulvinar (Stepniewska and Kaas, 1997). Some theories of the evolution of the pulvinar suggest that PIp and PIcm were a single nucleus that also included PIm. They subsequently split with the expansion of PIm, and differentiated from one another (Baldwin et al., 2017). If this actually occurred, and if titi monkeys are representative of an ancestral form of New World monkeys, then it is not surprising to see instances in titi monkeys where PIp and PIcm are bridged together along the ventral aspect of the inferior pulvinar under PIm (i.e. Fig. 7 and 8). Similar branching patterns, in both the ventral and dorsal aspects of PIp and PIcm have been reported for squirrel monkeys (Baldwin et al., 2017) using VGLUT2, and for most New World monkeys using calbindin (i.e. Stepniewska and Kaas, 1997; Stepniewska et al., 1999; 2000; Soares et al., 2001b; Warner et al., 2010).

Interestingly, PIcm has two separate bands of VGLUT2 protein expression (Fig. 8). This type of pattern is not present in squirrel monkeys (see Baldwin et al., 2017), but a similar pattern is observed in macaque monkeys (unpublished results, and see Balaram et al., 2013 Fig. 4d). It is unclear what this staining pattern means. It is thought that the VGLUT2 positive terminals within PIcm likely originate from inputs from the superior colliculus (Balaram et al., 2011; 2013; Baldwin et al., 2017). Thus, one question is whether the superior colliculus projections to PIcm terminate only in these two bands, or if there are also non-VGLUT2-expressing projections. Regardless, further studies using VGLUT2 staining patterns within PIcm of other New World monkeys will help to determine which of the two staining patterns are unique or shared features across New World monkeys. Such an understanding could provide insights into the functional implications of the two different types of staining patterns.

In summary, all New World monkeys have a seven-layered superior colliculus. While all New World monkeys examined have a lateral geniculate nucleus that contains two magnocellular layers and two parvocellular layers, the parvocellular layers split into separate leaflets in some species. Furthermore, the number, size, and chemical composition of the K layers is highly variable across New World monkeys, which is most apparent when comparing across species using tissue sections processed for Cb (Fig. 10). The general organization of the pulvinar is similar across all New World monkeys and contains clear inferior and lateral subdivisions. The presence of a “shell” has been somewhat controversial (see Stepniewska and Kaas, 1997), but it does seem clear that in titi monkeys there are at least four divisions of the inferior pulvinar (PIp, PIm, PIcm, PIcl), and a shell that is separate from the lateral pulvinar and PIcl.

Comparison to macaque monkeys and humans

Superior colliculus—The superior colliculus of macaque monkeys and humans is similar to that observed in New World monkeys and other primates and contains seven main layers. There may be subtle differences in the proportion of these layers in comparison to other primates, as the proportion of the superior colliculus dedicated to the superficial layers in macaques appears smaller than that in galagos (see Baldwin and Bourne, 2017). However, specific volumetric measurements have not been made.

Nissl, CO, Cb, Pv, and VGLUT2 stains have all been used to examine the superior colliculus of macaque monkeys (i.e. Mize and Luo, 1992; Balaram et al., 2013). Like titi monkeys, VGLUT2 staining in macaques appears to reflect retinal terminations patterns within the superficial layers of the SC (Pollack and Hickey, 1979; Balaram et al., 2013). However, the pattern of VGLUT2 label within the upper SGS of macaques is much patchier than what is observed in titi monkeys (Balaram et al., 2013; Figs. 3 and 4), and the changes in VGLUT2 staining patterns across the medial/lateral and rostral/caudal extent of the superior colliculus seem to be amplified relative to titi monkeys (Fig. 4). Finally, the contrast in staining patterns for CO, VGLUT2, and AChE, and the density differences in cells between the SGS, SO, and SGI borders is more robust in macaques than titi monkeys. The superior colliculus of humans has been studied using Pv and Cb, and staining patterns are similar to those observed in titi monkeys (Leuba and Saini, 1996; 1997).

Lateral geniculate nucleus—The lateral geniculate nucleus of macaque monkeys is well characterized as having six layers composed of two magnocellular and four parvocellular layers. This feature of organization of the lateral geniculate nucleus is different than that of New World monkeys where the number of parvocellular layers is variable (Fig. 10).

The LGN of macaques has been studied using the same histological stains as those used in the present study. Generally, the lateral geniculate nucleus of titi monkeys and macaques appear to be very similar with only a few subtle differences. Like titi monkeys, the location of the lamina observed in macaques is similar relative to the optic tract, with magnocellular layers located ventral to parvocellular layers and multiple K layers located between them, including between the external magnocellular layer and the optic tract. K1 of macaques is the most similar koniocellular layer to that observed in titi monkeys, having both dense

VGLUT2 staining and Cb+ cells and neuropil. In macaques, K1 receives dense SC projections with less dense patches of SC projections to other interlaminar layers (Stepniewska et al., 1999; Harting et al., 1991; Benevento and Rezak, 1976). It seems likely that K1 of titi monkeys would also receive dense SC projections similar to what is found in other New World monkeys (Harting et al., 1978; Harting et al., 1991; Stepniewska et al., 1999; 2000) and macaques.

Unlike titi monkeys, there are differences in the staining patterns of the magnocellular and parvocellular layers for CO, Pv, and VGLUT2 staining in macaques, with the magnocellular layers staining darker than the parvocellular layers (Jones and Hendry, 1989; Balaram et al., 2013). The interlaminar zones of macaques are also mostly devoid of Pv, while this is not the case in titi monkeys (Fig. 5). The interlaminar zones ventral to K1 all contain sparse VGLUT2 labeling, while in titi monkeys, patches of dense VGLUT2 terminals are also found in K2 (Figs. 5d and 6).

In the lateral geniculate nucleus of humans, six distinct laminae are present and consist of two magnocellular layers and two parvocellular layers that split into four interleaving parvocellular leaflets within some portions of the lateral geniculate nucleus (Andrews et al., 1997; Leuba and Saini, 1996; 1997). A small K1 is present ventral to ME in some portions of the lateral geniculate nucleus, but it does not extend throughout the entire rostral to caudal extent of the nucleus (Leuba and Saini, 1996). Similar to titi monkeys, Cb preparations of human lateral geniculate nucleus tissue reveal Cb+ cells scattered throughout the interlaminar zones, but Cb+ neuropil is absent, except in K1 (Leuba and Saini, 1996).

In summary, the lateral geniculate nucleus of macaques and humans is similar to that of titi monkeys, with only a few subtle differences. Some of these differences likely reflect changes in the subcortical driving inputs to the lateral geniculate nucleus (i.e. VGLUT2 staining properties in the K layers), and the importance of the magnocellular and parvocellular pathways.

Visual pulvinar—Cytoarchitectonic and immunohistochemical studies of the visual pulvinar have been well studied in macaque monkeys and include the same histological preparations studied in the current report (Gutierrez et al., 1995; Gray et al., 1999, Adams et al., 2000; Stepniewska et al., 2000; Balaram et al., 2013; Rovo et al., 2012). For the histological stains used in the current study, there were no significant differences between the inferior pulvinar of macaques and titi monkeys (Gutierrez et al., 1995; Gray et al., 1999; Stepniewska et al., 2000; Balaram et al., 2013). The main difference between macaques and titi monkeys is the seemingly increased density of Cb+ cells along the border of the medial and lateral pulvinar (compare Fig. 9b with Fig. 15 of Stepniewska and Kaas, 1997). Why this difference exists or the significance of these Cb+ cells in this region is unknown.

The architectonic characteristics of the human pulvinar have only been reported in a few limited studies (Cola et al., 1999, 2005). In these studies, AChE and CO were used to characterize the pulvinar. The staining patterns were similar to those of the current report; however, the borders of some of the subdivisions are different, and the authors report an absence of the P_{IP} division found in other primates (see Baldwin et al., 2017 for review).

Comparisons to tarsiers

Historically, tarsiers were grouped into a single prosimian clade with strepsirrhines; however, recent evidence suggests that the ancestors of tarsiers diverged early from the haplorrhine primates and formed their own distinct primate radiation (Fig. 1) (Perelman et al., 2011). Relevant studies on tarsiers are limited. However, because of their unique phylogenetic position, studies of tarsiers are important for distinguishing differences between strepsirrhines and haplorrhines.

Superior colliculus—Nissl, and CO preparations of the SC of tarsiers reveal a laminar pattern similar to other primates including titi monkeys (Collins et al., 2005a).

Lateral geniculate nucleus—The tarsier lateral geniculate nucleus contains two magnocellular layers and two parvocellular layers that are most distinguishable from one another using calbindin preparations (Collins et al., 2005a; Wong et al., 2010). Like titi monkeys, calbindin positive neuropil are found in K1. However, unlike titi monkeys, dense calbindin positive neuropil are also especially present within the interlaminar zones between MI and PI, and PI and PE (Fig. 10). Cb+ neuropil may also be present within K2, but the staining pattern is much weaker than K3 and K4 (see Collins et al., 2005a). In the tarsier, the parvocellular layers stain darkly for AChE, while the magnocellular layers and the interlaminar zone between MI and PI layers stain weakly (Mc Donald et al., 1993).

Visual Pulvinar—Both inferior and lateral divisions of the pulvinar have been identified in tarsiers (Collins et al., 2005a; Wong et al., 2010). Similar to titi monkeys, divisions of the inferior pulvinar are easily identified in Cb tissue preparations with PIp and PIcm containing dense Cb+ neuropil and cell bodies and PIm staining weakly (Collins et al., 2005a; Wong et al., 2010). The consistency in staining properties of the tarsier with other New World monkeys suggests that these divisions likely have similar functional roles in vision and were present in the ancestor of haplorrhines. The anatomical characteristics of both the lateral geniculate nucleus and the pulvinar are more similar to anthropoid primates than to strepsirrhines (see below), which provides further support that tarsiers are more closely related to anthropoid primates than to strepsirrhines.

Comparisons to strepsirrhines

The ancestors of strepsirrhines diverged early in primate evolution, prior to the divergence of all other anthropoid primates and tarsiers (Fig. 1). Thus, studies in species within this group are useful in determining what brain features are likely present in the common ancestor to all primates. Of the strepsirrhines, which include the lemurs, lorises, galagos, and pottos; galagos are the most well studied.

Superior colliculus—Histological properties of the superior colliculus of strepsirrhine primates are similar to those of other primates, including titi monkeys. Specifically, in galagos, the SGS contains densely packed cells and stains darkly for CO and AChE, while the SO is less cell-packed and stains weakly for AChE and CO (Balaram et al., 2011; Baldwin et al., 2013). VGLUT2 staining has only been studied in galagos. In these preparations, the upper SGS stains darkly and homogeneously for VGLUT2 protein

throughout the medial to lateral extent and does not have the patchy pattern observed in macaques (Balaram et al., 2013) or differences in the staining pattern across the medial/lateral or caudal/rostral extent observed in titi monkeys (Fig. 4).

Lateral geniculate nucleus—The lateral geniculate of galagos and other strepsirrhines can be divided into 6 layers, which consists of two parvocellular layers, two magnocellular layers, and two distinct koniocellular layers. Like titi monkeys, differentiation between parvocellular and magnocellular layers of the lateral geniculate nucleus in prosimians is not robust with CO or VGLUT2 preparations, yet these layers do stain more darkly than the K layers (Balaram et al., 2011; McDonald et al., 1993). Unlike titi monkeys, there are significant differences in the staining properties of the P and M layers of the lateral geniculate nucleus, with the M layers mostly staining weakly for AChE, while the P layers stain darkly (McDonald et al., 1993). This appears to be consistent across strepsirrhines regardless of diurnal, nocturnal, or diel lifestyles.

A distinguishing feature of the lateral geniculate nucleus of strepsirrhines is the prominence of the two K layers located between the internal and external parvocellular layers (Balaram et al., 2011; McDonald et al., 1993). These two distinct K layers are usually referred to as the internal (KI) and the external (KE) and are easily identified in Nissl preparations as two weakly staining bands of small cells (Balaram et al., 2011; McDonald et al., 1993). If a consistent nomenclature is maintained across the layers of the lateral geniculate nucleus with other primates, these two K layers could be considered part of K4, which runs between the parvocellular layers of other primates (Fig. 10). Thus, we refer to these two layers by a hybrid name of K4 internal (K4I) and K4 external (K4E), which represent the two visible layers within this interlaminar region.

In studies of galagos, VGLUT2 positive-terminals are present throughout the interlaminar zones including K1–3, similar to titi monkeys. Unlike titi monkeys, however, the most dense and prominent labeling is within the K4I and K4E layers between PI and PE (Balaram et al., 2011). The entire interlaminar/K4 zone between PI and PE also stains darkly for Cb (Diamond, 1993; Johnson and Casagrande, 1995). Whether the unique complexity of K4 in strepsirrhines was present in the common ancestor of primates or was lost in haplorrhines primates is unknown.

One reason why this difference is present may pertain to differences in the retina→SC→LGN pathways across primates. K4 receives dense projections from the superior colliculus in galagos (Baldwin et al., 2013) and it is thought that both W and Y (or koniocellular and parvocellular) retinal ganglion cells (RGC) project to the superior colliculus based on the morphology of the terminal projections (Feig et al., 1992). Further evidence for the presence of projections to the superior colliculus from parvocellular RGCs in galagos comes from V1 lesion studies where parvocellular RGCs remain intact in the retina after longstanding lesions (Weller et al., 1981). Further, the response properties of the cells within K4 of galagos are more similar to neuronal response properties of cells within the parvocellular layers than those of the cells in the magnocellular layers (Norton et al., 1988). If parvocellular retinal ganglion cells do indeed project to the superior colliculus in prosimians, and their information is passed onto the lateral geniculate nucleus by way of

superior colliculus projections to K4 of the lateral geniculate nucleus, it would make sense that K4 is much more prominent in these primates compared to other primates where parvocellular RGCs are not known to project to the superior colliculus.

Visual pulvinar—As in other primates, inferior and lateral divisions of the pulvinar can be identified in galagos. Although AChE and Cb have been useful in revealing subdivisions in the inferior pulvinar of both New World and Old World monkeys, such preparations are not robust markers for subdivisions in prosimian primates such as galagos (Wong et al., 2009; Baldwin et al., 2013). Recently, the possible homologues of PIP and PICM observed in haplorrhines has been revealed in galagos using VGLUT2 immunohistological staining (Baldwin et al., 2013; Baldwin et al., 2017). Like other primates, including titi monkeys, these divisions stain darkly for VGLUT2 protein, and this staining preparation may be a useful tool for revealing homologous divisions in all primates (Baldwin et al., 2017).

Summary

The superior colliculus seems relatively unchanged across primate lineages and even across mammals, except possibly for the proportions that the different layers within it occupy. Though the superior colliculus has been well-studied across primates, few architectonic studies with a wide variety of histological preparations have been conducted, especially within New World monkeys. VGLUT2 staining characteristics seem to mimic the projection patterns of retinal input within anthropoid primates and highlight differences in such projections across different primate lines with patchy or inconsistent patterns of projections across the superior colliculus in anthropoids vs. prosimians.

Despite the concept that the koniocellular pathway is an “old” visual pathway (Bishop 1959; Diamond et al., 1993), there are considerable differences in the comparative organization, size, known connections, and chemoarchitecture of the different K layers within primates (See Casagrande and Khaytin, 2009; also see Fig. 10). In macaque monkeys, tarsiers, and most new world monkeys, K1 and K3 are among the thickest layers and contain the greatest number of cells, while in galagos, the interlaminar zone between PE and PI (K4I and K4E) is the largest (Hendry and Yoshioka, 1994; Johnson and Casagrande, 1995; Xu et al., 2001). One of the reasons for these differences in the K layers could be the changes in visual input from the retina via the superior colliculus, which is most notable between prosimians and anthropoid primate lines. However, this hypothesis needs to be tested further. Differences in the density of SC projections to K layers are also apparent in New World vs. Old world monkeys with the densest SC projections to K1 and weaker projections to other K layers in macaques, while in New World monkeys SC projections are dense to K1, K2, and K3 and less dense to K layers between the parvocellular layers (when present) (Stepniewska et al., 1999; 2000).

Our understanding of the organization and evolution of the pulvinar, and especially divisions of the inferior pulvinar, has become clearer because of comparative studies using a number of histological stains across a number of different primate species (See Baldwin et al., 2017 for review). There are still questions about how many divisions are present within the visual pulvinar across different primates, and the existence of a “shell” division within the pulvinar

of anthropoids is not consistently reported (Cusick et al., 1993; Gutierrez et al., 1995; Stepniewska and Kaas; 1997; Kaas and Lyon, 2007; Lyon et al., 2010). In the present study, we show evidence for a shell based on histological staining properties, which are consistent with reports in other New World monkeys. A possible homologue may also be present in galagos (Baldwin et al., 2017). Further studies of the connection patterns to this region of the pulvinar would help resolve the issue. Finally, unlike our knowledge of the functional contributions of the magnocellular and parvocellular layers of the lateral geniculate nucleus (Schiller and Logothetis, 1990; Shapley, 1992; Casagrande, 1994; Casagrande and Kaas, 1994; Usrey and Reid, 2000), the functional roles of the different nuclei within the pulvinar are still not fully understood.

As a graduate student, Vivien Casagrande started her career in neuroscience studying the anatomy and function of the superior colliculus and later became well known for her work on anatomical studies of parallel visual pathways through the lateral geniculate nucleus. More recently, she was exploring the functional organization and anatomy of the pulvinar complex (i.e. Li et al., 2013). Vivien's insights through her comparative studies, and her examination of concurrent changes within subcortical and cortical visual brain structures across different primates and their close relatives, allowed her to make substantial insights into our understanding of the functional organization of the visual system as a whole. Her contributions have influenced the visual neuroscience community substantially, as evidenced by the reports in this special issue. The findings of the current report would have little context without her previous contributions.

Acknowledgments

This research was supported by a grant from NIH NINDS NS035103 to LK, and NIH NINDS F32 NS093721-01 to MLKB.

We dedicate this manuscript in memory of Dr. Vivien Casagrande. Vivien served on the thesis committees of both Leah and myself, and continued to provide invaluable advice after we graduated. Her love of science, drive, extraordinary anatomical skills, and critical insights were beyond reproach. She was our mentor in graduate school, and our friend and colleague as we progressed in our careers. Although her absence has left a hole in our lives, her scientific excellence, tenacity, and kindness still have the power to dazzle us all.

List of Abbreviations

AChE	Acetylcholinesterase
Cb	calbindin
Cb+	calbindin positive
cc	corpus callosum
CO	cytochrome oxidase
LGN	lateral geniculate nucleus
PAG	periaqueductal gray
PI	inferior pulvinar

PIcl	central lateral inferior pulvinar
PIcm	central medial inferior pulvinar
PIm	medial inferior pulvinar
PIp	posterior inferior pulvinar
PL	lateral pulvinar
PLdm	dorsomedial lateral pulvinar
PLvl	ventrolateral lateral pulvinar
PM	medial pulvinar
Pul	pulvinar
Pv	parvalbumin
Pv+	parvalbumin positive
s	shell division of the pulvinar
SAI	stratum album intermedium
SAP	stratum album profundum
SC	superior colliculus
SGP	stratum griseum profundum
SGS	stratum griseum superficial
uSGS	upper stratum griseum superficial
ISGS	lower stratum griseum superficial
SO	stratum opticum
SZ	stratum zonale
Thal	thalamus
V1	primary visual cortex, striate cortex
V2	secondary visual cortex
VGLUT2	vesicular glutamate transporter 2

References

- Adams MM, Hof PR, Gattass R, Webster MJ, Ungerleider LG. Visual cortical projections and chemoarchitecture of macaque monkey pulvinar. *J Comp Neurol.* 2000; 419(3):377–393. [PubMed: 10723012]
- Andrews TJ, Halpern SD, Purves D. Correlated size variations in human visual cortex, lateral geniculate nucleus, and optic tract. *J Neurosci.* 1997; 17(8):2859–2868. [PubMed: 9092607]

- Balaram P, Hackett TA, Kaas JH. Differential expression of vesicular glutamate transporters 1 and 2 may identify distinct modes of glutamatergic transmission in the macaque visual system. *J Chem Neuroanat.* 2013; 50–51:21–38. DOI: 10.1016/j.jchemneu.2013.02.007
- Balaram P, Isaamullah M, Petry HM, Bickford ME, Kaas JH. Distributions of vesicular glutamate transporters 1 and 2 in the visual system of tree shrews (*Tupaia belangeri*). *J Comp Neurol.* 2015; 523(12):1792–1808. DOI: 10.1002/cne.23727 [PubMed: 25521420]
- Balaram P, Takahata T, Kaas JH. VGLUT2 mRNA and protein expression in the visual thalamus and midbrain of prosimian galagos (*Otolemur garnettii*). *Eye Brain.* 2011; 2011(3):5–15. DOI: 10.2147/EB.S16998 [PubMed: 22984342]
- Baldwin MK, Balaram P, Kaas JH. Projections of the superior colliculus to the pulvinar in prosimian galagos (*Otolemur garnettii*) and VGLUT2 staining of the visual pulvinar. *J Comp Neurol.* 2013; 521(7):1664–1682. DOI: 10.1002/cne.23252 [PubMed: 23124867]
- Baldwin MK, Bourne JA. The evolution of subcortical pathways to the extrastriate cortex. In: Kaas, J., editor. *Evolution of nervous systems.* 2. Vol. 3. Elsevier; 2017. p. 165-185.
- Baldwin MK, Kaas JH. Cortical projections to the superior colliculus in prosimian galagos (*Otolemur garnettii*). *J Comp Neurol.* 2012; 520(9):2002–2020. DOI: 10.1002/cne.23025 [PubMed: 22173729]
- Baldwin MK, Wong P, Reed JL, Kaas JH. Superior colliculus connections with visual thalamus in gray squirrels (*Sciurus carolinensis*): evidence for four subdivisions within the pulvinar complex. *J Comp Neurol.* 2011; 519(6):1071–1094. DOI: 10.1002/cne.22552 [PubMed: 21344403]
- Baldwin MKL, Balaram P, Kaas JH. The evolution and functions of nuclei of the visual pulvinar in primates. *J Comp Neurol.* 2017; 525(15):3207–3226. DOI: 10.1002/cne.24272 [PubMed: 28653446]
- Bales KL, Arias Del Razo R, Conklin QA, Hartman S, Mayer HS, Rogers FD, ... Wright EC. Titi Monkeys as a Novel Non-Human Primate Model for the Neurobiology of Pair Bonding. *Yale J Biol Med.* 2017; 90(3):373–387. [PubMed: 28955178]
- Bishop GH. The relationship between nerve fiber size and sensory modality: phylogenetic implications of the afferent innervation of cortex. *Journal of Nervous and Mental Disease.* 1959; 128(2):89–114.
- Bourne JA, Rosa MG. Laminar expression of neurofilament protein in the superior colliculus of the marmoset monkey (*Callithrix jacchus*). *Brain Res.* 2003; 973(1):142–145. [PubMed: 12729963]
- Bridge H, Leopold DA, Bourne JA. Adaptive Pulvinar Circuitry Supports Visual Cognition. *Trends Cogn Sci.* 2016; 20(2):146–157. DOI: 10.1016/j.tics.2015.10.003 [PubMed: 26553222]
- Casagrande VA. A third parallel visual pathway to primate area V1. *Trends Neurosci.* 1994; 17(7): 305–310. [PubMed: 7524217]
- Casagrande VA, Diamond IT. Ablation study of the superior colliculus in the tree shrew (*Tupaia glis*). *J Comp Neurol.* 1974; 156(2):207–237. DOI: 10.1002/cne.901560206 [PubMed: 4424699]
- Casagrande VA, Kaas JH. The afferent, intrinsic, and efferent connections of primary visual cortex in primates. In: Peters, A., Rockland, KS., editors. *Cerebral cortex. Primary visual cortex in primates.* Vol. 10. New York: Plenum Press; 1994.
- Casagrande VA, Yazar F, Jones KD, Ding Y. The morphology of the koniocellular axon pathway in the macaque monkey. *Cerebral Cortex.* 2007; 17:2334–2345. [PubMed: 17215477]
- Casagrande VA, Khaytin, I. The evolution of parallel pathways in the brains of primates. In: Kaas, J., editor. *Evolution of Nervous systems.* Elsevier; 2009. p. 871-892.
- Cola MG, Gray DN, Seltzer B, Cusick CG. Human thalamus: neurochemical mapping of inferior pulvinar complex. *Neuroreport.* 1999; 10(18):3733–3738. [PubMed: 10716200]
- Cola MG, Seltzer B, Preuss TM, Cusick CG. Neurochemical organization of chimpanzee inferior pulvinar complex. *J Comp Neurol.* 2005; 484(3):299–312. DOI: 10.1002/cne.20448 [PubMed: 15739240]
- Collins CE, Hendrickson A, Kaas JH. Overview of the visual system of *Tarsius*. *Anat Rec A Discov Mol Cell Evol Biol.* 2005; 287(1):1013–1025. DOI: 10.1002/ar.a.20263 [PubMed: 16200648]
- Collins CE, Lyon DC, Kaas JH. Distribution across cortical areas of neurons projecting to the superior colliculus in new world monkeys. *Anat Rec A Discov Mol Cell Evol Biol.* 2005; 285(1):619–627. DOI: 10.1002/ar.a.20207 [PubMed: 15912524]

- Cusick CG, Scriptor JL, Darensbourg JG, Weber JT. Chemoarchitectonic subdivisions of the visual pulvinar in monkeys and their connectional relations with the middle temporal and rostral dorsolateral visual areas, MT and DLr. *J Comp Neurol.* 1993; 336(1):1–30. DOI: 10.1002/cne.903360102 [PubMed: 8254107]
- Diamond IT, Fitzpatrick D, Schmechel D. Calcium binding proteins distinguish large and small cells of the ventral posterior and lateral geniculate nuclei of the prosimian galago and the tree shrew (*Tupaia belangeri*). *Proc Natl Acad Sci U S A.* 1993; 90(4):1425–1429. [PubMed: 8434002]
- Dyer MA, Martins R, da Silva Filho M, Muniz JA, Silveira LC, Cepko CL, Finlay BL. Developmental sources of conservation and variation in the evolution of the primate eye. *Proc Natl Acad Sci U S A.* 2009; 106(22):8963–8968. DOI: 10.1073/pnas.0901484106 [PubMed: 19451636]
- Feig S, Van Lieshout DP, Harting JK. Ultrastructural studies of retinal, visual cortical (area 17), and parabigeminal terminals within the superior colliculus of *Galago crassicaudatus*. *J Comp Neurol.* 1992; 319(1):85–99. DOI: 10.1002/cne.903190109 [PubMed: 1592907]
- Fitzpatrick D, Itoh K, Diamond IT. The laminar organization of the lateral geniculate body and the striate cortex in the squirrel monkey (*Saimiri sciureus*). *J Neurosci.* 1983; 3(4):673–702. [PubMed: 6187901]
- Fleagle JG. Perspectives in primate evolution. *Evol Anthropol.* 2012; 21(6):207. doi: 10.1002/evan.21337 [PubMed: 23280917]
- Geneser-Jensen FA, Blackstad TW. Distribution of acetyl cholinesterase in the hippocampal region of the guinea pig. I. Entorhinal area, parasubiculum, and presubiculum. *Z Zellforsch Mikrosk Anat.* 1971; 114(4):460–481. [PubMed: 5550728]
- Goodchild AK, Martin PR. The distribution of calcium-binding proteins in the lateral geniculate nucleus and visual cortex of a New World monkey, the marmoset, *Callithrix jacchus*. *Vis Neurosci.* 1998; 15(4):625–642. [PubMed: 9682866]
- Gray D, Gutierrez C, Cusick CG. Neurochemical organization of inferior pulvinar complex in squirrel monkeys and macaques revealed by acetylcholinesterase histochemistry, calbindin and Cat-301 immunostaining, and *Wisteria floribunda* agglutinin binding. *J Comp Neurol.* 1999; 409(3):452–468. [PubMed: 10379830]
- Gutierrez C, Cusick CG. Area V1 in macaque monkeys projects to multiple histochemically defined subdivisions of the inferior pulvinar complex. *Brain Res.* 1997; 765(2):349–356. [PubMed: 9313911]
- Gutierrez C, Yaun A, Cusick CG. Neurochemical subdivisions of the inferior pulvinar in macaque monkeys. *J Comp Neurol.* 1995; 363(4):545–562. DOI: 10.1002/cne.903630404 [PubMed: 8847417]
- Harting JK, Casagrande VA, Weber JT. The projection of the primate superior colliculus upon the dorsal lateral geniculate nucleus: autoradiographic demonstration of interlaminar distribution of tectogeniculate axons. *Brain Res.* 1978; 150(3):593–599. [PubMed: 79427]
- Harting JK, Huerta MF, Frankfurter AJ, Strominger NL, Royce GJ. Ascending pathways from the monkey superior colliculus: an autoradiographic analysis. *J Comp Neurol.* 1980; 192(4):853–882. DOI: 10.1002/cne.901920414 [PubMed: 7419758]
- Harting JK, Huerta MF, Hashikawa T, van Lieshout DP. Projection of the mammalian superior colliculus upon the dorsal lateral geniculate nucleus: organization of tectogeniculate pathways in nineteen species. *J Comp Neurol.* 1991; 304(2):275–306. DOI: 10.1002/cne.903040210 [PubMed: 1707899]
- Hendry SH, Reid RC. The koniocellular pathway in primate vision. *Annu Rev Neurosci.* 2000; 23:127–153. DOI: 10.1146/annurev.neuro.23.1.127 [PubMed: 10845061]
- Hendry SH, Yoshioka T. A neurochemically distinct third channel in the macaque dorsal lateral geniculate nucleus. *Science.* 1994; 264(5158):575–577. [PubMed: 8160015]
- Hershkovitz. Origin, Speciation, and Distribution of the South American Titi Monkeys, Genus *Callicebus* (Family Cebidae, Platyrrhini). *Proceedings of the Academy of Natural Sciences of Philadelphia.* 1988; 140(1):240–272.
- Huerta MF, Harting JK. Sublamination within the superficial gray layer of the squirrel monkey: an analysis of the tectopulvinar projection using anterograde and retrograde transport methods. *Brain Res.* 1983; 261(1):119–126. [PubMed: 6839147]

- Jackson CP. The positional behavior of pygmy marmosets (*Cebuella pygmaea*) in northwestern Bolivia. *Primates*. 2011; 52(2):171–178. DOI: 10.1007/s10329-011-0237-7 [PubMed: 21360318]
- Jacobs GH. Primate photopigments and primate color vision. *Proc Natl Acad Sci U S A*. 1996; 93(2): 577–581. [PubMed: 8570598]
- Johnson JK, Casagrande VA. Distribution of calcium-binding proteins within the parallel visual pathways of a primate (*Galago crassicaudatus*). *J Comp Neurol*. 1995; 356(2):238–260. DOI: 10.1002/cne.903560208 [PubMed: 7629317]
- Jones, EG. *The Thalamus*. 2. Cambridge University Press; 2007.
- Jones EG, Hendry SH. Differential Calcium Binding Protein Immunoreactivity Distinguishes Classes of Relay Neurons in Monkey Thalamic Nuclei. *Eur J Neurosci*. 1989; 1(3):222–246. [PubMed: 12106154]
- Kaas, JH., Huerta, MF. The subcortical system of primates. In: Steklis, HD., editor. *Comparative primate biology*. New York: Wiley; 1988.
- Kaas JH, Huerta MF, Weber JT, Harting JK. Patterns of retinal terminations and laminar organization of the lateral geniculate nucleus of primates. *J Comp Neurol*. 1978; 182(3):517–553. DOI: 10.1002/cne.901820308 [PubMed: 102662]
- Kaas JH, Lyon DC. Pulvinar contributions to the dorsal and ventral streams of visual processing in primates. *Brain Res Rev*. 2007; 55(2):285–296. DOI: 10.1016/j.brainresrev.2007.02.008 [PubMed: 17433837]
- Kaas JH, Morel A. Connections of visual areas of the upper temporal lobe of owl monkeys: the MT crescent and dorsal and ventral subdivisions of FST. *J Neurosci*. 1993; 13(2):534–546. [PubMed: 8381166]
- Kaplan G, Rogers LJ. Head-cocking as a form of exploration in the common marmoset and its development. *Dev Psychobiol*. 2006; 48(7):551–560. DOI: 10.1002/dev.20155 [PubMed: 17016839]
- Koga A, Tanabe H, Hirai Y, Imai H, Imamura M, Oishi T, ... Hirai H. Co-Opted Megasatellite DNA Drives Evolution of Secondary Night Vision in Azara's Owl Monkey. *Genome Biol Evol*. 2017; 9(7):1963–1970. DOI: 10.1093/gbe/evx142 [PubMed: 28810713]
- Leuba G, Saini K. Calcium-binding proteins immunoreactivity in the human subcortical and cortical visual structures. *Vis Neurosci*. 1996; 13(6):997–1009. [PubMed: 8961531]
- Leuba G, Saini K. Colocalization of parvalbumin, calretinin and calbindin D-28k in human cortical and subcortical visual structures. *J Chem Neuroanat*. 1997; 13(1):41–52. [PubMed: 9271194]
- Li K, Patel J, Purushothaman G, Marion RT, Casagrande VA. Retinotopic maps in the pulvinar of bush baby (*Otolemur garnettii*). *J Comp Neurol*. 2013; 521(15):3432–3450. DOI: 10.1002/cne.23358 [PubMed: 23640865]
- Lin CS, Kaas JH. The inferior pulvinar complex in owl monkeys: architectonic subdivisions and patterns of input from the superior colliculus and subdivisions of visual cortex. *J Comp Neurol*. 1979; 187(4):655–678. DOI: 10.1002/cne.901870403 [PubMed: 114556]
- Lin CS, Kaas JH. Projections from the medial nucleus of the inferior pulvinar complex to the middle temporal area of the visual cortex. *Neuroscience*. 1980; 5(12):2219–2228. [PubMed: 7465053]
- Lund RD. Anatomic studies on the superior colliculus. *Invest Ophthalmol*. 1972; 11(6):434–441. [PubMed: 4624289]
- Lyon DC, Nassi JJ, Callaway EM. A disynaptic relay from superior colliculus to dorsal stream visual cortex in macaque monkey. *Neuron*. 2010; 65(2):270–279. DOI: 10.1016/j.neuron.2010.01.003 [PubMed: 20152132]
- Mangalam M, Frigaszy DM. Wild bearded capuchin monkeys crack nuts dexterously. *Curr Biol*. 2015; 25(10):1334–1339. DOI: 10.1016/j.cub.2015.03.035 [PubMed: 25936553]
- May PJ. The mammalian superior colliculus: laminar structure and connections. *Prog Brain Res*. 2006; 151:321–378. DOI: 10.1016/S0079-6123(05)51011-2 [PubMed: 16221594]
- McCrea RA, Gdowski GT. Firing behaviour of squirrel monkey eye movement-related vestibular nucleus neurons during gaze saccades. *J Physiol*. 2003; 546(Pt 1):207–224. [PubMed: 12509489]
- McDonald CT, McGuinness ER, Allman JM. Laminar organization of acetylcholinesterase and cytochrome oxidase in the lateral geniculate nucleus of prosimians. *Neuroscience*. 1993; 54(4): 1091–1101. [PubMed: 8393538]

- Mize RR, Luo Q. Visual deprivation fails to reduce calbindin 28kD or GABA immunoreactivity in the rhesus monkey superior colliculus. *Vis Neurosci.* 1992; 9(2):157–168. [PubMed: 1504025]
- Padberg J, Franca JG, Cooke DF, Soares JG, Rosa MG, Fiorani M Jr, ... Krubitzer L. Parallel evolution of cortical areas involved in skilled hand use. *J Neurosci.* 2007; 27(38):10106–10115. DOI: 10.1523/JNEUROSCI.2632-07.2007 [PubMed: 17881517]
- Percival KA, Koizumi A, Masri RA, Buzas P, Martin PR, Grunert U. Identification of a pathway from the retina to koniocellular layer K1 in the lateral geniculate nucleus of marmoset. *J Neurosci.* 2014; 34(11):3821–3825. DOI: 10.1523/JNEUROSCI.4491-13.2014 [PubMed: 24623761]
- Perelman P, Johnson WE, Roos C, Seuanez HN, Horvath JE, Moreira MA, ... Pecon-Slattery J. A molecular phylogeny of living primates. *PLoS Genet.* 2011; 7(3):e1001342.doi: 10.1371/journal.pgen.1001342 [PubMed: 21436896]
- Pollack JG, Hickey TL. The distribution of retino-collicular axon terminals in rhesus monkey. *J Comp Neurol.* 1979; 185(4):587–602. DOI: 10.1002/cne.901850402 [PubMed: 109475]
- Rovo Z, Ulbert I, Acsady L. Drivers of the primate thalamus. *J Neurosci.* 2012; 32(49):17894–17908. DOI: 10.1523/JNEUROSCI.2815-12.2012 [PubMed: 23223308]
- Schiller PH, Logothetis NK. The color-opponent and broad-band channels of the primate visual system. *Trends Neurosci.* 1990; 13(10):392–398. [PubMed: 1700509]
- Shapley R. Developments in vision. *Science.* 1992; 256(5065):1837–1838. DOI: 10.1126/science.256.5065.1837-a
- Soares JG, Botelho EP, Gattass R. Distribution of calbindin, parvalbumin and calretinin in the lateral geniculate nucleus and superior colliculus in *Cebus apella* monkeys. *J Chem Neuroanat.* 2001; 22(3):139–146. [PubMed: 11522436]
- Soares JG, Gattass R, Souza AP, Rosa MG, Fiorani M Jr, Brandao BL. Connectional and neurochemical subdivisions of the pulvinar in *Cebus* monkeys. *Vis Neurosci.* 2001; 18(1):25–41. [PubMed: 11347814]
- Soares JG, Mendez-Otero R, Gattass R. Distribution of NADPH-diaphorase in the superior colliculus of *Cebus* monkeys, and co-localization with calcium-binding proteins. *Neurosci Res.* 2003; 46(4):475–483. [PubMed: 12871769]
- Soares JG, Rosado De Castro PH, Fiorani M, Nascimento-Silva S, Gattass R. Distribution of neurofilament proteins in the lateral geniculate nucleus, primary visual cortex, and area MT of adult *Cebus* monkeys. *J Comp Neurol.* 2008; 508(4):605–614. DOI: 10.1002/cne.21718 [PubMed: 18383052]
- Solomon SG, White AJ, Martin PR. Extraclassical receptive field properties of parvocellular, magnocellular, and koniocellular cells in the primate lateral geniculate nucleus. *J Neurosci.* 2002; 22(1):338–349. [PubMed: 11756517]
- Springer MS, Meredith RW, Gatesy J, Emerling CA, Park J, Rabosky DL, ... Murphy WJ. Macroevolutionary dynamics and historical biogeography of primate diversification inferred from a species supermatrix. *PLoS One.* 2012; 7(11):e49521.doi: 10.1371/journal.pone.0049521 [PubMed: 23166696]
- Stepniewska I, Kaas JH. Architectonic subdivisions of the inferior pulvinar in New World and Old World monkeys. *Vis Neurosci.* 1997; 14(6):1043–1060. [PubMed: 9447687]
- Stepniewska I, Qi HX, Kaas JH. Do superior colliculus projection zones in the inferior pulvinar project to MT in primates? *Eur J Neurosci.* 1999; 11(2):469–480. [PubMed: 10051748]
- Stepniewska I, Qi HX, Kaas JH. Projections of the superior colliculus to subdivisions of the inferior pulvinar in New World and Old World monkeys. *Vis Neurosci.* 2000; 17(4):529–549. [PubMed: 11016573]
- Tigges J, O'Steen WK. Termination of retinofugal fibers in squirrel monkey: a reinvestigation using autoradiographic methods. *Brain Res.* 1974; 79(3):489–495. [PubMed: 4213996]
- Tigges J, Tigges M. Distribution of retinofugal and corticofugal axon terminals in the superior colliculus of squirrel monkey. *Invest Ophthalmol Vis Sci.* 1981; 20(2):149–158. [PubMed: 7461921]
- Tigges M, Tigges J. The retinofugal fibers and their terminal nuclei in *Galago crassicaudatus* (primates). *J Comp Neurol.* 1970; 138(1):87–101. DOI: 10.1002/cne.901380107 [PubMed: 5412721]

- Usrey WM, Reid RC. Visual physiology of the lateral geniculate nucleus in two species of new world monkey: *Saimiri sciureus* and *Aotus trivirgatus*. *J Physiol*. 2000; 523(Pt 3):755–769. [PubMed: 10718753]
- Visalberghi E, Giulia S, Frigaszy D, Boesch C. Percussive tool use by Tai Western chimpanzees and Fezenda Boa Vista bearded capuchin monkeys: a comparison. *Phil Trans R Soc B*. 2017; 370 (20140351).
- Warner CE, Goldshmit Y, Bourne JA. Retinal afferents synapse with relay cells targeting the middle temporal area in the pulvinar and lateral geniculate nuclei. *Front Neuroanat*. 2010; 4:8.doi: 10.3389/neuro.05.008.2010 [PubMed: 20179789]
- Weller RE, Kaas JH. Parameters affecting the loss of ganglion cells of the retina following ablations of striate cortex in primates. *Vis Neurosci*. 1989; 3(4):327–349. [PubMed: 2487111]
- Weller RE, Kaas JH, Ward J. Preservation of retinal ganglion cells and normal patterns of retinogeniculate projections in prosimian primates with long-term ablations of striate cortex. *Invest Ophthalmol Vis Sci*. 1981; 20(2):139–148. [PubMed: 6780485]
- Weller RE, Kaas JH, Wetzel AB. Evidence for the loss of X-cells of the retina after long-term ablation of visual cortex in monkeys. *Brain Res*. 1979; 160(1):134–138. [PubMed: 102413]
- White AJ, Solomon SG, Martin PR. Spatial properties of koniocellular cells in the lateral geniculate nucleus of the marmoset *Callithrix jacchus*. *J Physiol*. 2001; 533(Pt 2):519–535. [PubMed: 11389209]
- Wong P, Collins CE, Baldwin MK, Kaas JH. Cortical connections of the visual pulvinar complex in prosimian galagos (*Otolemur garnetti*). *J Comp Neurol*. 2009; 517(4):493–511. DOI: 10.1002/cne.22162 [PubMed: 19795374]
- Wong P, Collins CE, Kaas JH. Overview of Sensory Systems of *Tarsius*. *International Journal of Primatology*. 2010; 31(6):1002–1031.
- Wong-Riley M. Changes in the visual system of monocularly sutured or enucleated cats demonstrable with cytochrome oxidase histochemistry. *Brain Res*. 1979; 171(1):11–28. [PubMed: 223730]
- Xu X, Bosking W, Sary G, Stefansic J, Shima D, Casagrande V. Functional organization of visual cortex in the owl monkey. *J Neurosci*. 2004; 24(28):6237–6247. DOI: 10.1523/JNEUROSCI.1144-04.2004 [PubMed: 15254078]
- Xu X, Ichida JM, Allison JD, Boyd JD, Bonds AB, Casagrande VA. A comparison of koniocellular, magnocellular and parvocellular receptive field properties in the lateral geniculate nucleus of the owl monkey (*Aotus trivirgatus*). *J Physiol*. 2001; 531(Pt 1):203–218. [PubMed: 11179404]

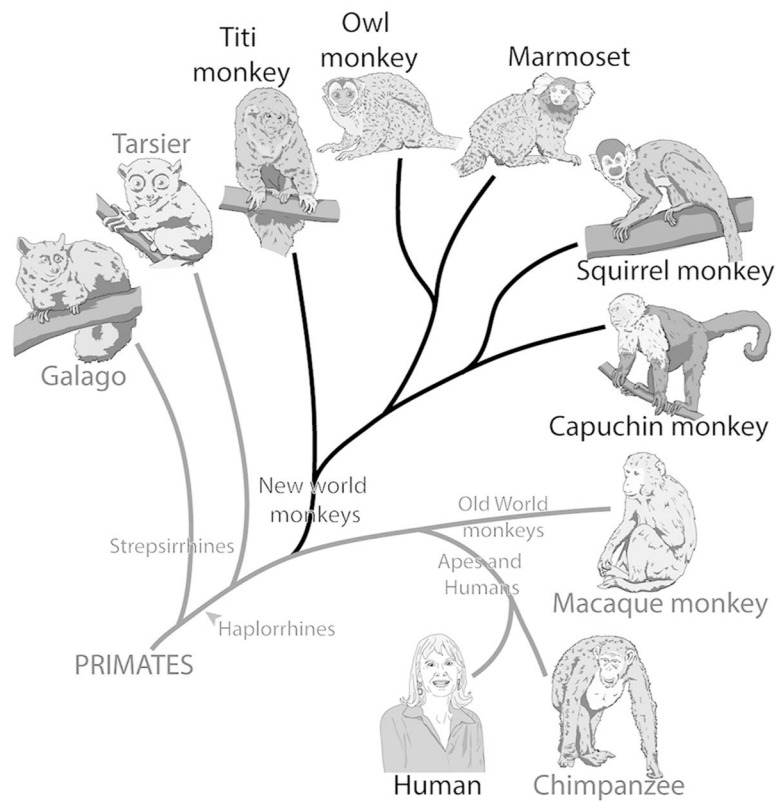


Figure 1.

A cladogram showing the phylogenetic relationship of various extant primates. Each branch point indicates when species shared a common ancestor. Titi monkeys are New World monkeys and share a common ancestor with the rest of New World monkeys, but their lineage branched off prior to the major New World monkey radiation.

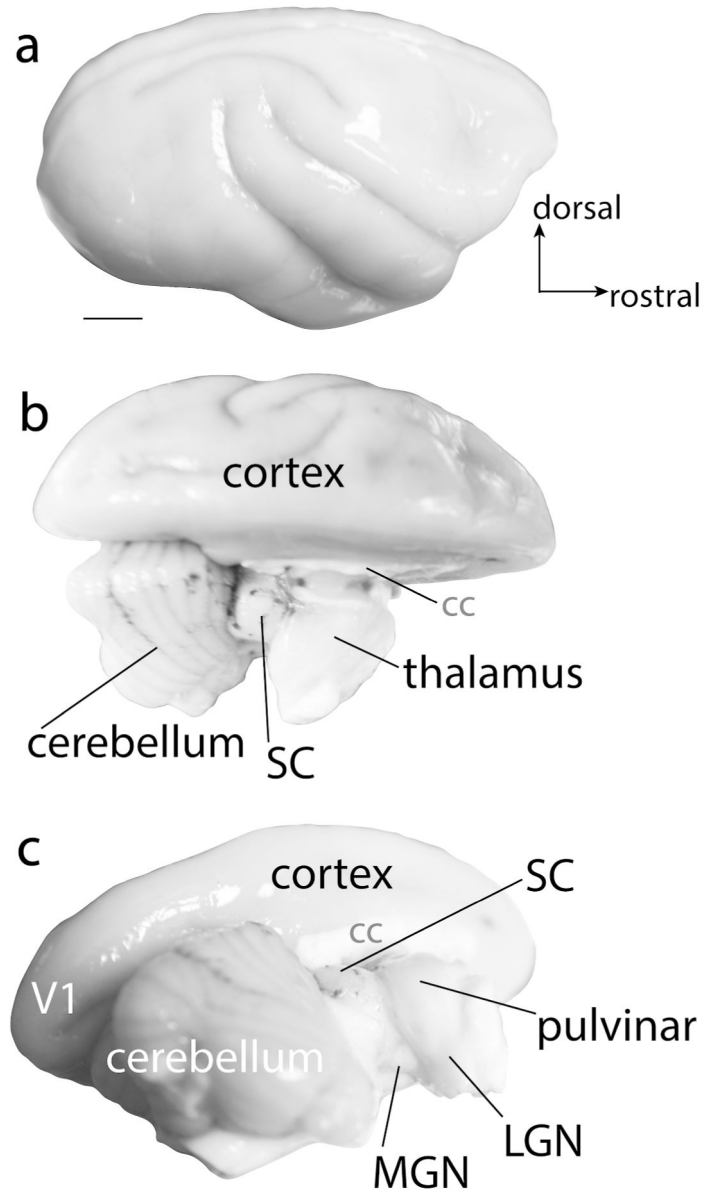


Figure 2.

The gross anatomy of the brain of a titi monkey. **a** is a lateral view of the right hemisphere of the titi monkey brain. **b** is a dorsal view of the titi monkey brain with the right hemisphere removed, revealing subcortical structures including the cerebellum, superior colliculus (SC), and dorsal thalamus. **c** is a caudolateral view of the titi monkey brain with the right hemisphere removed and shows the location of the pulvinar, lateral geniculate nucleus (LGN), and medial geniculate nucleus (MGN). Scale bar is 5 mm.

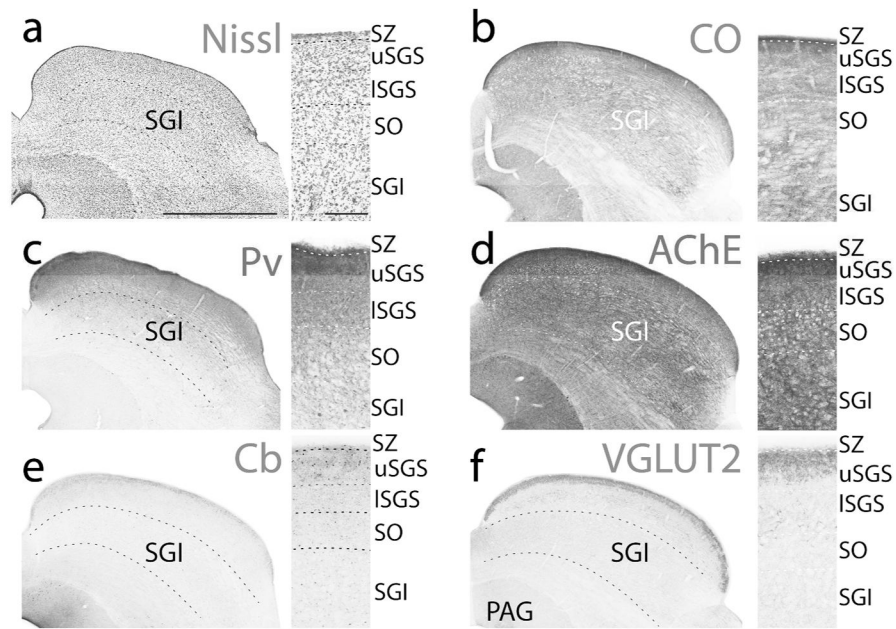


Figure 3. Different histological stains showing the laminar organization of the superior colliculus of titi monkeys. Coronal sections of the superior colliculus stained for Nissl substance (**a**), cytochrome oxidase (CO, **b**), parvalbumin (Pv, **c**), acetylcholinesterase (AChE, **d**), calbindin (Cb, **e**), and vesicular glutamate transporter 2 (VGLUT2, **f**). Images are taken from two cases (**a** and **c** from 16–246, while **b**, **d–f** are from 16–191). Boxes to the right are enlarged images of the superficial layers of the SC for each stain, with laminar borders outlined with dashed white lines. Dorsal is up, lateral is to the right, scale bar for the large coronal sections (left) are 1 mm, while the scale bar for the close-up boxes are 0.25 mm).

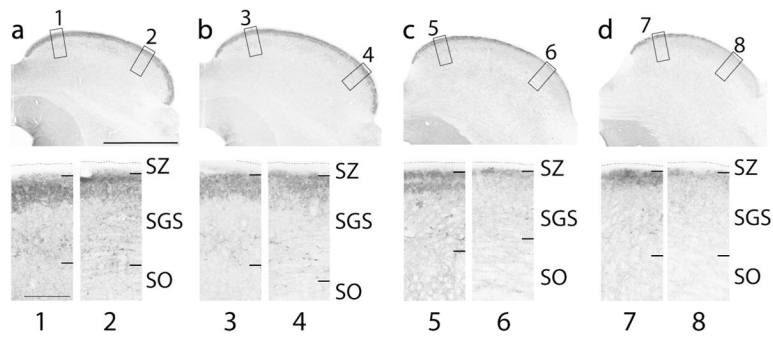


Figure 4. Vesicular glutamate transporter 2 staining throughout the caudal (left: **a**) to rostral (right: **d**) extent of the superior colliculus highlighting the heterogeneity of the upper SGS. Low-power coronal sections stained for VGLUT2 are in the top row. High-power views of the medial and lateral portions of the superior colliculus demonstrating the laminar patterns of staining of the superficial layers (bottom row). Numbers below the high-power images on the bottom row correspond to the numbers next to the boxes in the top row. Black dashed lines indicate the dorsal border of the stratum zonale (SZ). Dorsal is up, lateral is to the right, scale bar is 2 mm for the top row and 0.25 mm for the bottom row. Section images are all from case 16–191.

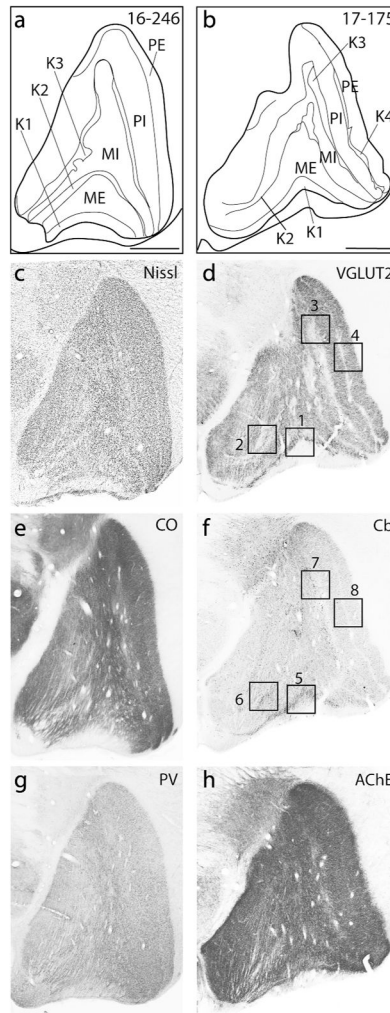


Figure 5. Coronal sections processed for different histological preparations used to reveal the laminar organization of the lateral geniculate nucleus of titi monkeys (**a** and **b**). Coronal sections were processed for Nissl (**c**), vesicular glutamate transporter 2 (VGLUT2: **d**), cytochrome oxidase (CO: **e**), calbindin (Cb: **f**), parvalbumin (Pv: **g**), and acetylcholinesterase (AChE: **h**). Enlarged images of the boxed regions in the Cb and VGLUT2 images are presented in Figure 6. Dorsal is up, lateral is to the right, scale bars are 1 mm. **a**, **c**, **e**, **g** are from case 16–246, while **b**, **d**, **f**, and **h** are from case 17–175.

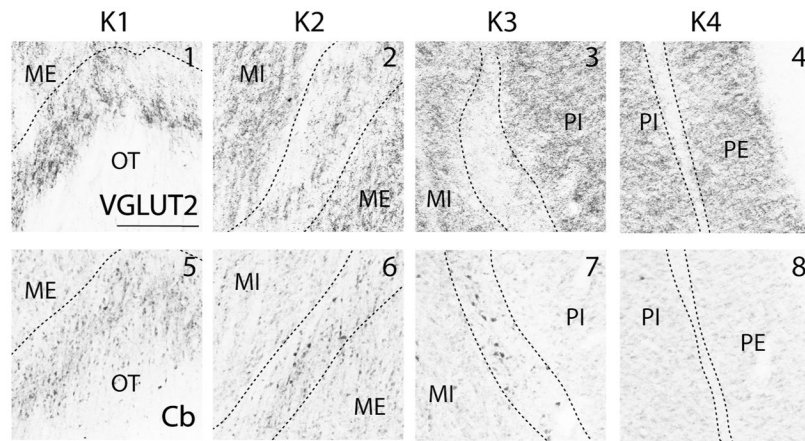


Figure 6.

Enlarged photomicrographs of the boxed regions in Figure 5 showing vesicular glutamate transporter 2 (VGLUT2: top row) and calbindin (Cb: bottom row) immunohistochemical staining patterns within different K layers of the lateral geniculate nucleus. Numbers at the top of boxes correspond to the numbers by boxes in Figure 5. Dashed black lines indicate the borders between lamina. Dorsal is up, lateral is to the right, scale bar is 0.25 mm.

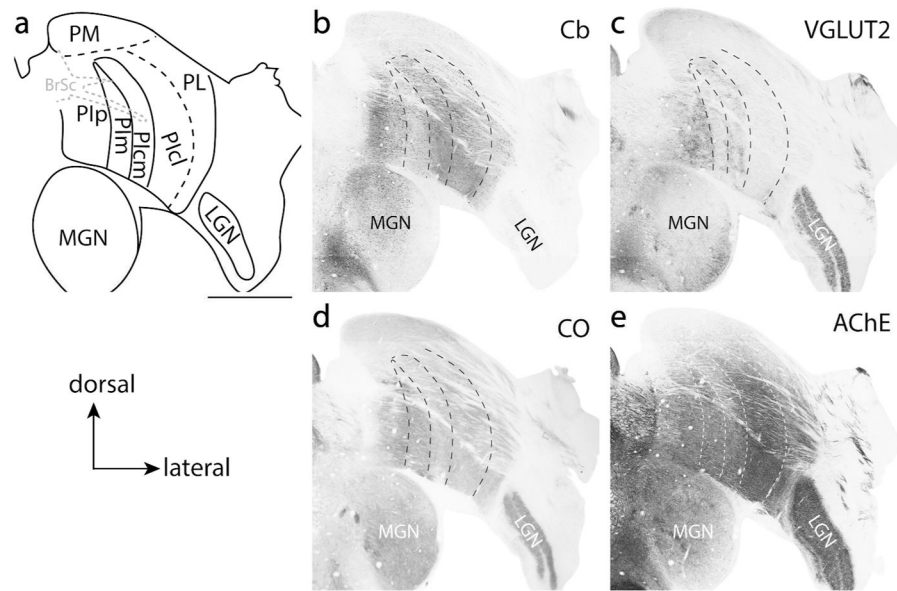


Figure 7. Subdivisions of the pulvinar complex of titi monkeys. Sections are taken from a more caudal location of the pulvinar. **(a)** Illustration of the borders of the pulvinar revealed with coronal sections processed for different histological preparations. Adjacent sections processed for calbindin (Cb: **b**), vesicular glutamate transporter 2 (VGLUT2: **c**); cytochrome oxidase (CO: **d**) and acetylcholinesterase (AChE: **e**), used to reveal different subdivisions of the pulvinar. Some borders of subdivisions are indicated with dashed lines. The combination of multiple stains is most useful for defining borders. All sections are from case 16–191. Scale bar is 2 mm.

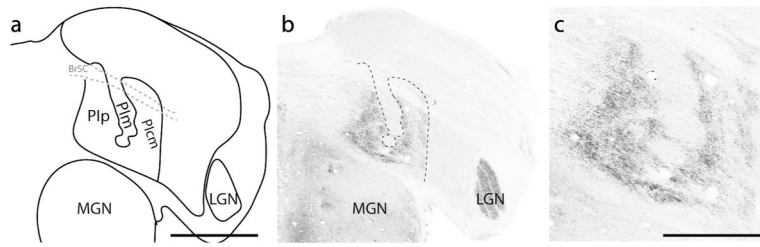


Figure 8.

Coronal sections through the caudal pulvinar. **(a)** shows the locations of thalamic borders and subdivisions derived from sections stained for vesicular glutamate transporter 2 (VGLUT2) **(b)**. The borders of the inferior posterior (PIp), the inferior medial (PIIm), and the inferior caudal medial (PICm) divisions of the inferior pulvinar (PI) are readily visible with VGLUT2 staining. Both PIp and PICm stain darkly for VGLUT2 while PIIm stains weakly. Two bands of VGLUT2 staining can be seen within PICm. Note that PIp and PICm seem to merge or bridge together at the ventral aspect of the inferior pulvinar and that there are bands of VGLUT2 positive label connecting PIp and PICm through PIIm. Dashed lines highlight the borders of PIp, PIIm, and PICm. Far right panel **(c)** is a close-up digital image of PIp, PIIm, and PICm. Dorsal is up, lateral is to the right. Scale bar is 2 mm for **a** and 1 mm for **c**.

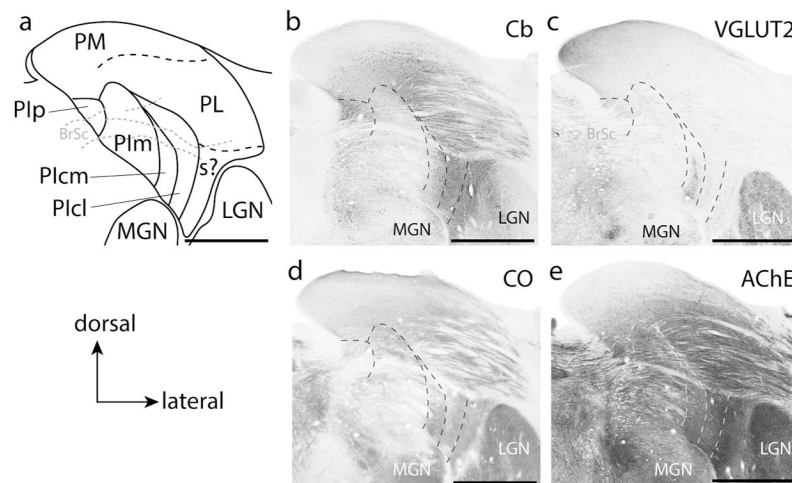


Figure 9. Subdivisions of the pulvinar complex in titi monkeys in a more rostral location to that shown in Figure 7. **(a)** Illustration of the borders of the pulvinar revealed in coronal sections processed for different histological preparations. “s?” indicate the possible location of the shell division of the pulvinar. Adjacent sections processed for calbindin (Cb: **b**), vesicular glutamate transporter 2 (VGLUT2: **c**); cytochrome oxidase (CO: **d**) and acetylcholinesterase (AChE: **e**), used to reveal different subdivisions of the pulvinar. The dashed lines indicate the location of some subdivision borders. Scale bar is 2 mm.

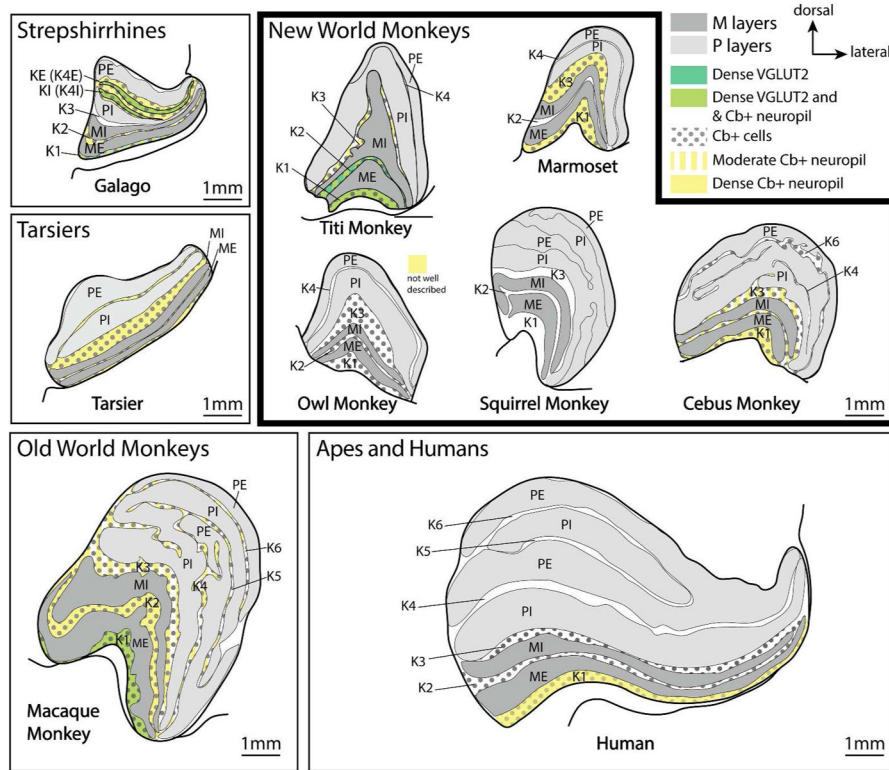


Figure 10. Summary of the organization of the lateral geniculate nucleus across different primate lines with examples including prosimians such as galagos and tarsiers, New World monkeys including titi monkeys, owl monkeys, marmosets, squirrel monkeys, and cebus monkeys, an Old World macaque monkey, and a human. While there are differences in the amount of the LGN devoted to the P versus M layers and the number of K layers, the basic structure of the LGN has been preserved across all primates. Magnocellular layers are highlighted in dark gray, while parvocellular layers are highlighted in light gray. The calbindin (cells = black dots, and neuropil are highlighted in yellow) and dense VGLUT2 staining properties of the K layers are highlighted. VGLUT2 has only been studied in galagos and macaque monkeys. Calbindin staining has not been well studied in squirrel monkeys (to the best of our knowledge). Though VGLUT2 terminals are present in other K layers, we have only highlighted those layers with dense VGLUT2 staining. All drawings are presented at the same scale.

Table 1

Case Overview

Case #	Brain structures processed	Plane of cut	Number of series and histological stains
16-191 <i>age:</i> 3.5 years <i>sex:</i> male <i>weight:</i> 1.2 kg	Thalamus and brainstem	Coronal (50 μ m)	CO AChE VGLUT2 Cb (1 series saved for another experiment)
16-246 <i>age:</i> 3.5 years <i>sex:</i> female <i>weight:</i> 1 kg	Thalamus and brainstem	Coronal (50 μ m)	CO Nissl Pv (2 series saved for another experiment)
17-175 <i>age:</i> 12.5 years <i>sex:</i> male <i>weight:</i> 1.1 kg	Thalamus and brainstem	Coronal (50 μ m)	CO AChE VGLUT2 Pv Cb

Author Manuscript

Author Manuscript

Author Manuscript

Author Manuscript

Table 2

Antibody characterizations

Antigen	Primary antibody	Secondary antibody	Normal serum
Vesicular glutamate transporter 2 (VGLUT2)	Monoclonal anti-VGLUT2 produced in mouse (Millipore) Catalog # MAB5504 RRID: AB_287552 Concentration: 1:5000	Polyclonal biotinylated horse anti-mouse IgG (Vector Labs) Catalog # BA-2000 RRID: 2313581 Concentration: 1:500	Horse serum (Sigma-Aldrich) Catalog # H1138
Calbindin D28k (Cb)	Monoclonal mouse anti-Cb D28k (Swant) Catalog # 300 RRID: AB_10000347 Concentration: 1:5000	Biotinylated horse anti-mouse IgG (Vector Labs) Catalog # BA-2000 RRID: 2313581 Concentration: 1:500	Horse serum (Sigma-Aldrich) Catalog # H1138
Parvalbumin (Pv)	Monoclonal anti-Pv produced in mouse (Sigma-Aldrich) Catalog # P3088 RRID: AB_477329 Concentration: 1:2000	Biotinylated horse anti-mouse IgG (Vector Labs) Catalog # BA-2000 RRID: 2313581 Concentration: 1:500	Horse serum (Sigma-Aldrich) Catalog # H1138